

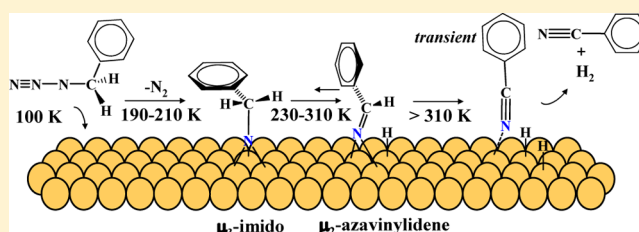
Capture of Bridging Imido and Azavinylidene Intermediates Engaged in Nitrogen Functionality Changes from Primary Azide to Nitrile on a Copper Surface

Cheng-Hung Cheng, Pao-Tao Yu, Kuo-Chen Ma, Yu-Chun Wang, Shin-Mou Wu, and Chao-Ming Chiang*

Department of Chemistry, National Sun Yat-Sen University, Kaohsiung 80424, Taiwan

S Supporting Information

ABSTRACT: Various nitrogen-based bridging ligands at the sites of a Cu(111) surface, including μ_3 -imido and μ_2 -azavinylidene species, have been identified by surface-sensitive spectroscopies and density functional theory (DFT) calculations. The isolated intermediates demonstrate how several metal atoms acting in concert can usher the conversion from a primary azide into a nitrile end-product. The collection of mechanistic details, the N–N₂ bond scission, the sequential β -hydrogen eliminations, and the alterations of the NC unsaturation, illustrates rich information about structures and transformations of N-donor ligands.



I. INTRODUCTION

Many transformations in heterogeneous catalysis involve the creation and modification of metal surface-bound unsaturated hydrocarbon functionalities, such as ethynyl ($\text{C}\equiv\text{CH}_2\text{R}$), vinyl ($\text{CH}=\text{CHR}$), vinylidene ($\text{C}=\text{CHR}$), acetylene ($\text{HC}\equiv\text{CR}$), and acetylide ($\text{C}\equiv\text{CR}$). To characterize the dehydrogenation, hydrogenation, and hydrogen-migration pathways among these species, one approach is to prepare them by adsorption of molecular precursors onto well-defined surfaces, then key mechanistic features in more complex conversion processes can be emulated.^{1–6} Nitrogenous multiple-bond analogues to these hydrocarbon reactive species encompass imido ($\text{M}\equiv\text{NR}$), imine ($\text{M}=\text{NHR}$), azavinylidene ($\text{M}=\text{NCH}_2\text{R}$), acimidoyl ($\text{M}=\text{NCH}_2\text{R}$), and nitrile ($\text{M}\equiv\text{NR}$) whose linkages to the metal are through nitrogen instead of carbon. However, because of the lack of readily available precursors, the roadmap for systematic interconversions within this family of ligands remains largely unexplored by surface scientists.

Organic azides ($\text{R}'\text{N}_3$) are known to undergo reactions with a metal center to transfer the nitrene $\text{R}'\text{N}$ group, rendering nitrene/imido complexes ($\text{M}\equiv\text{NR}'$) and the release of dinitrogen (N_2).⁷ We sought to extend this chemistry to metal surfaces by adsorbing benzylazide (PhCH_2N_3) on a copper (111) single crystal surface to deliver $\text{Cu}\equiv\text{NCH}_2\text{Ph}$, comparable to a metal-bound ethynyl, or hopefully other accessible dehydrogenated species. Copper is focused since copper-catalyzed aziridination of unsaturated organic substrates (the nitrogen analogue of epoxidation) has been conceived to proceed via a putative Cu–nitrene intermediate.⁸ The close-packed fcc (111) template further provides the 3-fold bridging sites where the valence of the desired nitrene/imido species can

be satisfied by interacting with several metal atoms at once. Here, we report on a sequence of surface events involving changes of the nitrogen functionality from a primary azide (PhCH_2N_3) to a nitrile (PhCN) identified by experimental surface analytic techniques and complementary density functional theory (DFT) calculations.

II. EXPERIMENTAL METHODS

The majority of the experiments were performed in an ultrahigh vacuum (UHV) chamber evacuated by a combination of ion and turbomolecular pumps. A base pressure below 1.0×10^{-10} Torr was reached after baking. The chamber was equipped with an ion sputtering source for surface cleaning, a triple-filter quadrupole mass spectrometer for detecting residual gases as well as desorbing species from the surface, and reflection absorption infrared spectroscopy (RAIRS) for collecting surface vibrational spectra. The Cu(111) single crystal (MaTeck, 99.999%) was attached to a heating element, mounted on a manipulator with capabilities for resistive heating to 1100 K and active cooling to 100 K by liquid nitrogen. A chromel–alumel thermocouple, whose junction was wedged into a hole in the side of the crystal, was used to measure the surface temperature. Programmed heating was achieved by a PID controller to ramp the temperature in a regulated fashion. The temperature-programmed desorption (TPD) experiments were usually started by exposing the Cu(111) crystal to the sample vapors at 100 K, and the surface was then elevated to 950 K with a linear rate of 2 K/s. Upon heating, multiple-ion

Received: July 26, 2013

Revised: September 8, 2013

Published: September 11, 2013

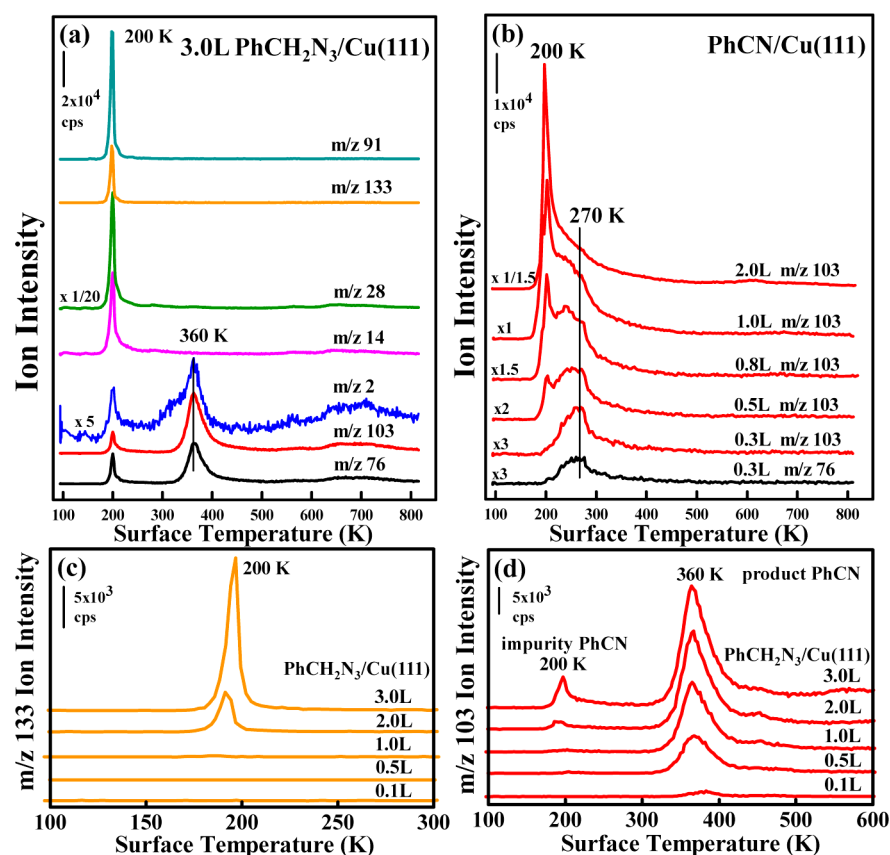


Figure 1. (a) Multiplex TPD spectra measured after adsorbing 3.0 L benzylazide on Cu(111) at 100 K. (b) Control TPD spectra for various exposures of Cu(111) to benzonitrile. (c,d) Trends of m/z 133 and 103 TPD signals as a function of benzylazide exposure.

signals and temperatures were collected synchronously. RAIRS was performed by taking the infrared beam from an FTIR spectrometer and focusing it at grazing incidence (85°) through a ZnSe wire-grid polarizer and a KBr window onto the Cu(111) in the UHV chamber. The reflected IR beam was then passed through a second KBr window and refocused on a liquid nitrogen cooled HgCdTe detector. All spectra corresponded to the average of 512 scans at 4 cm^{-1} resolution and were ratioed against the background spectra from the clean metal surface. The X-ray photoemission spectra (XPS) were recorded in a separate UHV chamber connected to a wide-range (10–1500 eV) spherical grating monochromator beamline at National Synchrotron Radiation Research Center in Hsinchu, Taiwan. Commercially available benzylazide (Alfa Aesar, 94%, highest grade available) and benzonitrile (Aldrich, 99.9%) were purified by several cycles of freeze–pump–thaw prior to use. Gas exposures were quoted as Langmuirs (L), uncorrected for ionization gauge sensitivity and collimator gain factor.

III. COMPUTATIONAL METHODS

The DFT calculations were carried out using the B3LYP functional^{9,10} as implemented in Gaussian09.¹¹ A relativistic LANL2DZ effective core potential (ECP) and a 6-31G basis set were used for the Cu cluster and the nitrogen-containing organic species, respectively. The Cu(111) surface was modeled by a two-layer Cu₂₅(18, 7) cluster where 18 and 7 represent the numbers of the surface and the subsurface layer atoms, respectively. The top layer containing 18 copper atoms was chosen to accommodate the large phenyl ring. The overall cluster size was a compromise between accuracy and cost in

modeling all the adsorbate/surface complexes involved. The copper clusters were fixed at a lattice constant of 2.556 Å. The nitrogen-containing ligands were first placed (not fixed) at the core hcp site with trial Cu–N bond distances of 2.0 Å to start the calculations. All geometries were optimized fully without symmetry constraints. Frequency calculations were performed to confirm the nature of the stationary points and to obtain zero-point energies. The frequencies given were corrected by a recommended scaling factor of 0.96 to compensate for the absence of anharmonicity in this type of computations.¹²

IV. RESULTS AND DISCUSSION

As illustrated in Figure 1a, following the adsorption of 3.0 L ($1\text{ L} = 10^{-6}\text{ Torr sec}$) benzylazide on Cu(111) at 100 K, multiplex TPD survey shows *two* major desorption channels with peak maxima at 200 and 360 K, respectively. The 200 K state reveals rapid azide decomposition to extrude molecular nitrogen, evidenced by the concurrent mass-to-charge ratio (m/z) 28 (N_2^+) and 14 (N^+) ion signals. In addition, desorption of intact molecules is characterized by m/z 133 (parent ion $\text{C}_7\text{H}_7\text{N}_3^+$) and 91 (C_7H_7^+ , base peak for the compound), together with secondary signals from m/z 2 (H_2^+), 103 ($\text{C}_7\text{H}_5\text{N}^+$), and 76 (C_6H_4^+). It is worth noting that the electron impact fragmentation pattern of benzylazide is devoid of the contribution from m/z 103, and an extraneous m/z 103 peak reproducibly showed up in our mass spectra when the sample was admitted to the chamber. The presence of benzonitrile, with m/z 103 and 76 being its two most abundant ions, as impurity was suspected (see Figure S1, Supporting Information, and the standard mass spectra documented in NIST Chemistry

WebBook). To confirm this assignment, pure benzonitrile was directly adsorbed on Cu(111) at 100 K and diagnosed by TPD. The high exposure data in Figure 1b indeed exhibits the liberation of condensed PhCN with a peak at ~ 200 K; however, a wide shoulder that extends to 350 K indicates that even monolayer PhCN (see the 0.3 L m/z 103 and 76 data with the peak maximum at 270 K) should depart by 350 K. The 360 K state in Figure 1a is highlighted by a broad H_2 evolution as well as an independent set of m/z 103 and 76 profiles whose integrated intensity ratio $I_{76}/I_{103} \approx 2/3$ duplicates the result of that obtained from the pure PhCN desorption at 270 K seen in Figure 1b. The temperature difference of the TPD peak maxima (360 vs 270 K) implicates that this channel represents conversion of benzylnitrile into benzonitrile by surface reactions. Figure 1c shows that the m/z 133 molecular desorption commences above 1.0 L below which the adsorbed $PhCH_2N_3$ should all undergo surface-assisted transformations, supported by the fact that the yield of product PhCN at 360 K takes off at coverage as low as 0.1 L and levels off at ~ 3.0 L, as shown in Figure 1d.

Adsorption onto Cu(111) appears to activate $PhCH_2N_3$ under mild conditions (<200 K) toward N–N₂ bond rupture, presumably affording benzylnitrile groups ($R'N$ where R' is $PhCH_2$) on the surface. To track the surface intermediate(s) en route to the terminal product, X-ray photoelectron spectra (XPS) were measured in a separate chamber at the Taiwan synchrotron facilities. Results from an exposure of 0.5 L $PhCH_2N_3$ in that chamber are selected to reveal both physisorbed and chemisorbed species. In Figure 2a, after

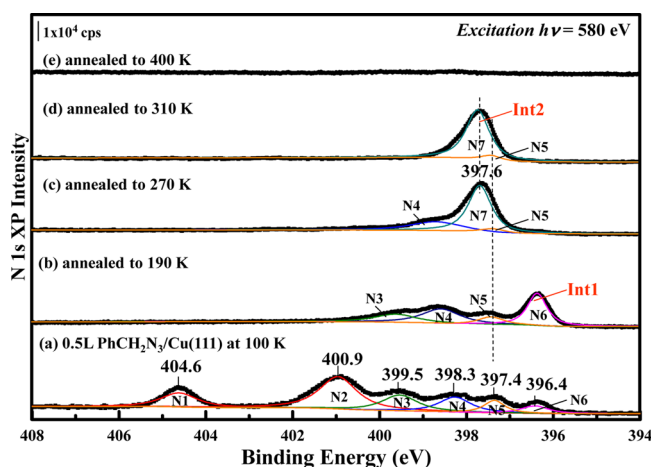


Figure 2. N 1s XP spectra obtained after annealing Cu(111) pre-exposed to 0.5 L of $PhCH_2N_3$ at 100 K to the indicated temperatures. Shirley baselines are applied and line shapes are fitted with 80% Lorentzian + 20% Gaussian.

deconvolution at least six peaks at binding energies (BEs) 404.6, 400.9, 399.5, 398.3, 397.4, and 396.4 eV (marked as N1–N6) are obtained in the N 1s region. N1 and N2 confirm the presence of the starting $PhCH_2N_3$,¹³ evidenced by the $\sim 1:2$ ratio of the integrated areas of these two components where the higher BE peak corresponds to the relatively electron-deficient middle N atom of the azido group ($-N^--N^+\equiv N$ or $-N=N^+-N^+$). N3, N4, and N5 in Figure 3a (same as Figure 2a) are believed to originate from the coadsorbed impurity PhCN molecules (with various bonding modes), substantiated by the three distinct N 1s features found at the similar BE positions in the spectrum (see Figure 3b) acquired after dosing 0.5 L pure

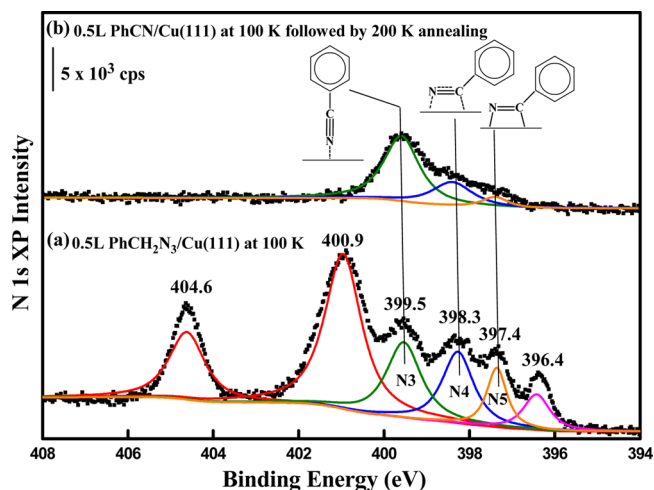


Figure 3. (a) N 1s XPS measured after exposing Cu(111) to 0.5 L benzylnitrile at 100 K. There exist at least six components after curve fitting. (b) N 1s XPS obtained after annealing Cu(111) pre-exposed to 0.5 L of benzonitrile at 100 to 200 K.

PhCN onto Cu(111) at 100 K followed by 200 K annealing (preventing the spectrum from being overwhelmed by the multilayer signals). Benzonitrile on Pd surfaces was reported to give three N 1s peaks: the component at 399.5 eV corresponds to condensed PhCN as well as weakly bonded η^1 -species through nitrogen lone-pair, while the features at 398.0 (between sp and sp^2) and 397.4 eV (sp^2) are assigned to η^2 -modes with different degree of rehybridization of the CN group.¹⁴

The relatively large peak areas of the impurity PhCN in Figure 2a may be explained by its higher sticking probability as opposed to the reactant. As for the smallest N6 component, because prior study has established a correlation between N 1s binding energy and formal metal–nitrogen bond order in metal amido, imido, and nitrido complexes, namely, a trend of $BE(M-N) > BE(M=N) > BE(M\equiv N)$,¹⁵ this peak at 396.4 eV is attributable to a $M\equiv NR'$ type intermediate (denoted as Int1). Annealing to 190 K clearly increases the intensity of the N6 peak concomitant with N1 and N2 disappearance in Figure 2b, suggesting substantial azide-to-Int1 conversion and elimination of any excessive molecular species. Some weakly bonded PhCN is also removed upon heating, displayed by the reduced N3 peak. Further annealing to 270 K results in a dominant feature at 397.6 eV, which might involve a different species (marked as N7) besides N5 due to its upshifted BE and the ascending intensity that correlates closely with the depletion of N6 (see Figure 2c). Formation of another discrete surface intermediate (Int2) is strongly implied. Meanwhile, a fair amount of PhCN impurity is now gone except for certain tightly bound N4 and N5. It is worth noting that the integrated peak area of N6 in Figure 2b appears not quite enough to account for all of the N7 in Figure 2c unless some of the coexisting PhCN (N3, N4, and N5) can be converted into N7 as well.¹⁶ Int2 (N7) is almost the single species remaining after annealing to 310 K as shown in Figure 2d. The steps at higher temperatures evolve PhCN product, leaving behind a featureless N 1s spectrum in Figure 2e.

The identities of Int1 and Int2 can be revealed by surface-sensitive RAIRS combined with DFT calculations. In Figure 4, physisorbed benzylnitrile on Cu(111) is first checked by the measured RAIR spectrum, which is quite similar to compound's

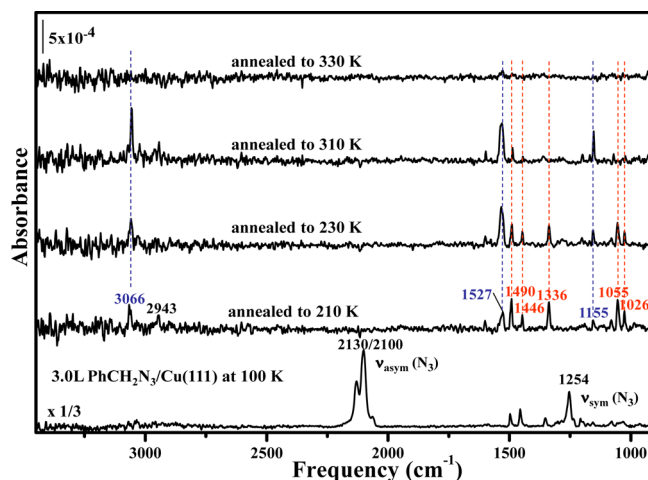


Figure 4. RAIR spectra after exposing Cu(111) to 3.0 L PhCH₂N₃ at 100 K, followed by annealing to the indicated temperatures.

liquid phase spectrum, featured by intense N₃ asymmetric stretching mode at 2130/2100 cm⁻¹ and the symmetric stretch around 1254 cm⁻¹.¹⁷ The C≡N stretching frequency (~2200 cm⁻¹) for impurity PhCN might be masked by the large azide signals. The N₃ bands disappear after annealing to 210 K (around the N₂ TPD peak temperature), and several different IR bands are observed, suggesting that new species are formed at the expense of the azido functionality. It is known that vibrational spectra for submonolayer coverage of benzonitrile on metal surfaces are relatively featureless (see Figure S2 in the Supporting Information);¹⁸ therefore, interference from the PhCN impurity is not a concern in interpreting the RAIR spectra. Here, eight major vibration bands, 3066, 1527, 1490, 1446, 1336, 1155, 1055, and 1026 cm⁻¹, are clearly visible, and their intensities vary as a function of temperature. Specifically, one set of peaks (1490, 1446, 1336, 1055, and 1026 cm⁻¹) is diminishing or even vanishing, while the other set (3066, 1527, and 1155 cm⁻¹) is rising from 210, via 230, to 310 K. Such development in the RAIRS mirrors the XPS annealing results, consolidating the interpretation that there exist two kinds of intermediates, and the former set of IR peaks characterizes Int1, while the latter set corresponds to Int2. Coexistence of both sets of IR features indicates that the 210 K annealing in fact generates an equilibrium mixture of Int1 and Int2, with the former being the prevailing species. However, at higher temperatures Int2 becomes predominant as the IR signals of Int1 fade out. Annealing to 330 K must readily trigger the successive reactions to dispose of the vibration features of the entire spectrum.

Int1 (N6) is very likely to be a Cu≡NCH₂Ph intermediate on Cu(111) following N₂ split-off (PhCH₂N–N≡N_(ad) → PhCH₂N_(ad) + N_{2(g)}). Gaussian DFT calculations were executed with a structure guessed as a “PhCH₂N” unit bound to a rigid Cu₂₅(18, 7) cluster where 18 and 7 represent the numbers of the surface and the subsurface layer atoms, respectively.¹⁹ The optimized geometrical parameters were employed to compute the vibrational frequencies corrected by a scaling factor of 0.96 and plotted by adding Lorentzian line shapes with a bandwidth of 4 cm⁻¹. The simulated IR spectrum is juxtaposed with the experimental spectrum for comparison. As illustrated in Figure 5a (experimental) and b (theoretical), reasonable conformity (by neglecting peaks at 1527 and 1155 cm⁻¹, which stand for Int2) is achieved by Cu₂₅N–CH₂Ph (see Scheme 1 for the

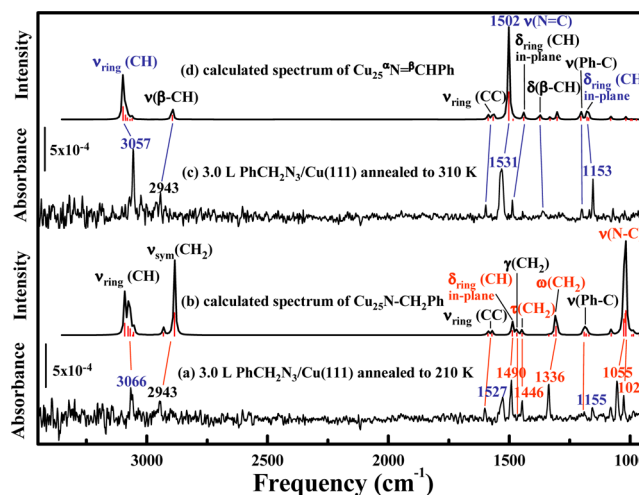


Figure 5. (a,c) Experimental RAIR spectra collected after exposing Cu(111) to 3.0 L PhCH₂N₃ at 100 K, followed by annealing at 210 and 310 K, respectively. (b,d) Calculated spectra derived from structure-optimized N–CH₂Ph and N=CHPh units bound to a Cu₂₅ cluster shown in Schemes 1 and 2

structure). Notably, the N–CH₂Ph nitrene unit is nearly symmetrically bound to the metal framework in a multinuclear fashion, namely, a triply bridging mode at a location near the 3-fold *hcp* hollow site, with the Cu–N bond lengths being 1.93, 1.93, and 1.91 Å, somewhat longer than those (1.84–1.89 Å) reported for μ₃-phenylimido groups in [Cu₂₄(NPh)₁₄]⁴⁺ and [Cu₁₂(NPh)₈]⁴⁺ clusters.²⁰ The N–C axis is almost perpendicular to the surface (4° from surface normal) with a distance of 1.48 Å (consistent with an NC single bond). The phenyl ring lies flat with a tilt angle about 27° relative to the surface. The band assignments built upon animations of the computed normal modes are annotated in Figure 5b. In particular, the pronounced doublet peak at 1055/1026 cm⁻¹ can be assigned to the ν(N–C) mode. The band splitting is a result of in-phase and out-of-phase couplings with the ring CH bending motions. On the basis of surface selection rule, it proves quite reasonable that besides the ν(N–C) stretch, the ω(CH₂) wagging motion at 1336 cm⁻¹ and τ(CH₂) twist at 1446 cm⁻¹ emerge as additional strong IR bands for their oscillating dipole moments are normal to the surface, whereas the modes involving dynamic dipole moments almost parallel to the surface, such as ν_{sym}(CH₂), ν_{ring}(CC), γ(CH₂) scissor, and ν(Ph–C) stretch, are rather weak or even undetectable experimentally. Nitrenes contain a monovalent nitrogen atom surrounded by only a sextet of electrons, so they might invite the migration of a group from the adjacent carbon to nitrogen in association with a CN double-bond formation to generate imines, i.e., PhCH₂N → PhC(H)=NH (1,2-hydrogen shift) or PhCH₂N → H₂C=NPh (1,2-phenyl shift). In fact, benzylazide complexes of iridium (III) were found to undergo N₂ expulsion followed by 1,2-H shift to give *N*-protio imine complexes.²¹ Therefore, adsorption structures as well as IR spectra of these viable intermediates, including Cu–N(H)=CHPh and Cu–N(Ph)=CH₂, were also calculated by DFT and shown in Figure 6b,c. The computed spectra bear little resemblance to our experimental data (Figure 6a). Particularly, the lack of definitive signals diagnostic of ν(N=C) lends no support to these rearranged forms of nitrene. It is thus safe to reject the imine-type intermediacy.

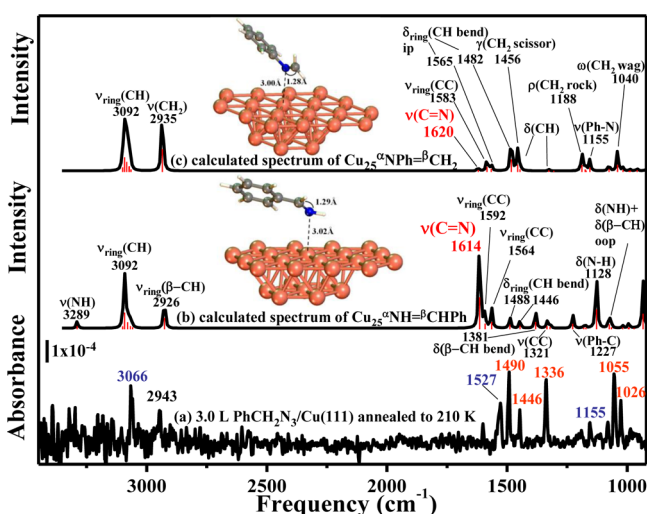
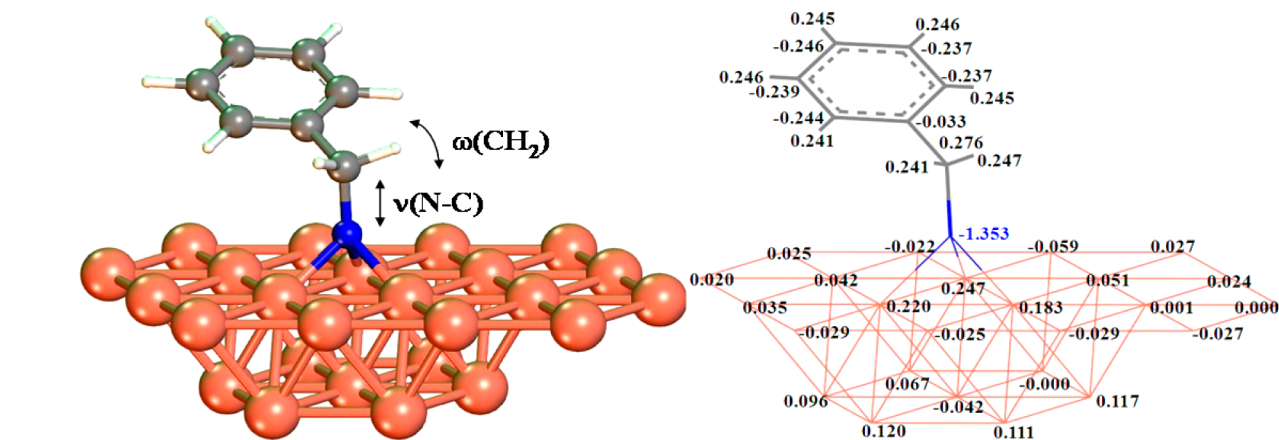
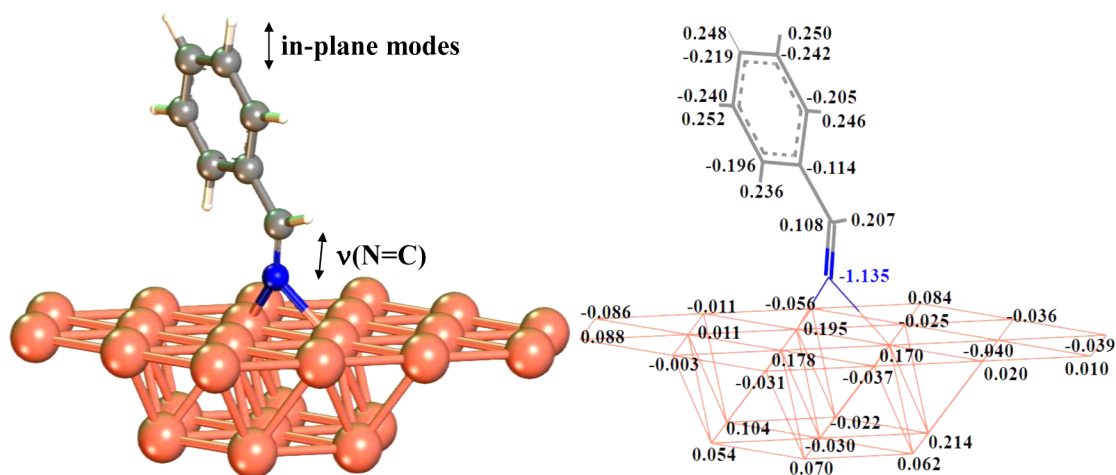
Scheme 1. Optimized $\text{Cu}_{25}(18,7)\text{N}-\text{CH}_2\text{Ph}$ Structure

Figure 6. (b,c) Optimized $\text{Cu}_{25}(18,7)\text{N}(\text{H})=\text{CHPh}$ (N -protio imine) and $\text{Cu}_{25}(18,7)\text{N}(\text{Ph})=\text{CH}_2$ (N -phenyl imine) structures and their theoretically predicted IR spectra in comparison with (a) the experimental spectrum, indicative of the surface intermediate (Int1) at 210 K after loss of N_2 from benzylazide.

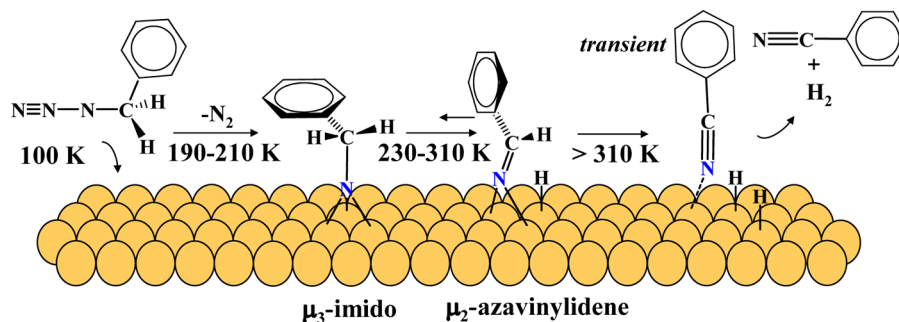
Natural population analysis (NPA) implemented in the Gaussian code reveals the atomic charges on the nitrogen and

the three nearest copper atoms in the $\text{Cu}_{25}\text{N}-\text{CH}_2\text{Ph}$ framework to be $-1.353e$ and $(+0.247e, +0.220e, \text{ and } +0.183e)$, shown in Scheme 1. For counterbalance to ligand's negative charge, adoption of the high coordination mode is accountable. A subtle difference between a metal-imido or metal-nitrene complex ($\text{M}\equiv\text{NR}'$) often depends on whether the NR' moiety is negatively charged or neutral, respectively. The strong ionic character (net charge on the $\text{N}-\text{CH}_2\text{Ph}$ group is $-1.153e$) suggests that the major intermediate (Int1) arrested at 210 K is better described as a copper benzyliimido species.

Int2, a separate nitrogen-containing species, is presumably derived mainly from Int1 as evidenced by the transition where N7 ($\text{BE} = 397.6 \text{ eV}$) in XPS and characteristic RAIRS bands ($3066, 1527, \text{ and } 1155 \text{ cm}^{-1}$) grows with the decline of N6 ($\text{BE} = 396.4 \text{ eV}$) and vibration features at $1490, 1446, 1336, \text{ and } 1055/1026 \text{ cm}^{-1}$. Abstraction of the hydrogen atoms at the carbon β to the metal for copper benzyliimido (Int1) must be considered along the path to the ultimate PhCN . Albeit unprecedented for imido ligands, the β -hydrogen eliminations from heteroatom alkoxo and amido transition-metal complexes wherein the α -atom is O or N are facile.^{22,23} Thus, $\text{Cu}=\text{N}=\text{CHPh}$, a vinylidene-like species, is the logical intermediate linking imido to nitrile. In principle, this $\text{Cu}\equiv\text{N}-\beta\text{CH}_2-\text{Ph} \rightarrow \text{Cu}=\text{N}=\text{CHPh} + \text{Cu}-\text{H}$ reaction would be supported by the disappearance of the $\nu(\text{N}-\text{C})$ and $\omega(\text{CH}_2)$ absorptions

Scheme 2. Optimized $\text{Cu}_{25}(18,7)\text{N}=\text{CHPh}$ Structure

Scheme 3. Proposed Reaction Mechanism



(readily confirmed by the vanishing 1055/1026 and 1336 cm^{-1} peaks from Figure 5a–c) and the appearance of a new band signature of the $\text{N}=\text{C}$ stretch. Is the most prominent 1531 cm^{-1} band observed in Figure 5c assignable to the anticipated $\nu(\text{N}=\text{C})$ mode? Again complementary DFT calculations were performed on the $\text{Cu}_{25}(18,7)$ -bound $\text{N}=\text{CHPh}$ unit in order to elucidate the experimental IR spectra. It turned out that the optimized N-donor ligand structure is $\mu_2\text{-N}=\text{CHPh}$, as shown in Scheme 2. The two metal centers are bridged by this azavinylidene moiety, with $\text{Cu}-\text{N}$ contacts being 1.97 and 1.98 Å. The NC axis is not entirely upright, and the tilt angle is $\sim 12^\circ$ relative to the surface normal. The NC bond distance of 1.30 Å is a bit longer than that typical of a NC double bond (1.28 Å); this is reflected in the relatively low frequency of $\nu(\text{N}=\text{C})$ vibration at 1502 cm^{-1} (red-shifted by at least 100 cm^{-1} in contrast to the normal $\text{N}=\text{C}$ stretch) in the computed spectrum for $\text{Cu}_{25}\text{N}=\text{CHPh}$ (Figure 5d), which nevertheless demonstrates a decent match with the pronounced experimental peak at 1531 cm^{-1} in Figure 5c. Other sharp and intense experimental vibration features at 3057 and 1153 cm^{-1} in Figure 5c can be ascribed to the common in-plane type ring CH stretching $\nu_{\text{ring}}(\text{CH})$ and bending $\delta_{\text{ring}}(\text{CH})$ modes, thus in support of the orientation with the phenyl group in a stand-up geometry. The $\nu(\beta\text{-CH})$ peak predicted by theory but almost illegible in Figure 5c is due to the small bond inclination relative to the surface ($\sim 29^\circ$). DFT calculations also forecast a switch from -1.353e for imido nitrogen to -1.135e for azavinylidene (See Scheme 2), which agrees well with the observed BE shift from 396.4 (N6) to 397.6 eV (N7). The core-level shift toward higher value is generally expected when electron density at the excitation center drops.

The removal of the remaining β -hydrogen in the azavinylidene intermediate (Int2) must occur above 310 K but below 330 K (see Figure 4), suggesting a higher activation barrier for the second β -hydrogen elimination process, $\text{Cu}=\text{N}=\text{CHPh} \rightarrow \text{Cu}-\text{N}\equiv\text{CPh} + \text{Cu}-\text{H}$. This can be rationalized by the fact that the rigid $\text{N}=\text{C}$ hinders the bond rotation to a well-accepted transition state with a coplanar arrangement of the α -nitrogen, the β -carbon, the β -hydrogen, and the metal center. Yet, such an adverse effect may be alleviated by the softened NC double bond and the presence of adjacent surface metal atoms (metal cooperativity), resulting in reactivity not routinely expected. The very broad H_2 TPD profile at ~ 360 K in Figure 1a also suggests this β -elimination step occurs with diverse rates depending on the actual sites. The outcome for the slower second β -hydrogen elimination would incur the NC triple bond formation. However, the RAIR spectrum at 330 K shows no signs of the cyano group. Hence, we interpret that the resultant $\text{PhC}\equiv\text{N}$ is weakly coordinated

and exists as a transient (elusive) species, which quickly desorbs when created (recall that straightforward PhCN desorption takes place at only 270 K).

V. CONCLUSIONS

In summary, the sound evidence presented above allows us to describe a reaction path where adsorption to the metal surface activates the primary azide (RCH_2N_3) toward stepwise dehydrogenations (β -hydrogen eliminations) and renders isolation at the μ_3 -imido and μ_2 -azavinylidene stages, as depicted in Scheme 3.

Cluster-bound NC multiple-bond systems often demonstrate a great diversity of interactions than is possible in mononuclear organometallic complexes: for instance, reversible ligand transformations of $\text{N}-\text{C} \leftrightarrow \text{N}=\text{C} \leftrightarrow \text{N}\equiv\text{C}$ were achieved on M_3 clusters (Fe_3 , Os_3 , and Ru_3),^{24–26} and these results from homogeneous catalysis research hinted how the heterogeneously catalyzed reactions proceed.²⁷ Our ability to realize the entire imido-azavinylidene-cyano sequence on an extended metal structure by using an azide precursor establishes a good example for the cluster-surface analogy. Imido and azavinylidene intermediates are catalytically relevant species in aziridination⁸ and ammoxidation.²⁸ We show they are reactive enough to interconvert but stable enough to be characterized on a model catalyst surface. Certain aspects of the purported ligand chemistry in solution are thus mimicked, and the garnered spectroscopic information (IR and XPS) may serve as useful references for other material systems.

■ ASSOCIATED CONTENT

Supporting Information

Mass spectral evidence for PhCN impurity; RAIR spectra of multilayer and monolayer PhCN adsorbed on $\text{Cu}(111)$. This material is available free of charge via the Internet at <http://pubs.acs.org>.

■ AUTHOR INFORMATION

Corresponding Author

*(C.-M.C.) E-mail: cmc@mail.nsysu.edu.tw. Phone: (+886) 7-5253939. Fax: (+886) 7-5253908.

Notes

The authors declare no competing financial interest.

■ ACKNOWLEDGMENTS

We thank the financial support from the National Science Council of the Republic of China under Contract No. 101-2113-M-110-011-MY2. We are grateful to the National Center for High-Performance Computing for computer time and

facilities. We also thank Dr. Y.-W. Yang and Dr. L.-J. Fan for their assistance on the XPS measurements.

REFERENCES

- (1) Deng, R.; Herceg, E.; Trenary, M. Identification and Hydrogenation of C_2 on Pt(111). *J. Am. Chem. Soc.* **2005**, *127*, 17628–17633.
- (2) Harris, J. J. W.; Florin, V.; Campbell, C. T.; King, D. A. Surface Products and Coverage Dependence of Dissociative Ethane Adsorption on Pt{110}-(1 × 2). *J. Phys. Chem. B* **2005**, *109*, 4069–4075.
- (3) Azad, S.; Kaltchev, M.; Stacchiola, D.; Wu, G.; Tysoe, W. T. On the Reaction Pathway for the Hydrogenation of Acetylene and Vinylidene on Pd(111). *J. Phys. Chem. B* **2000**, *104*, 3107–3115.
- (4) Zaera, F.; Bernstein, N. On the Mechanism for the Conversion of Ethylene to Ethylidyne on Metal Surfaces: Vinyl Halides on Pt(111). *J. Am. Chem. Soc.* **1994**, *116*, 4881–4887.
- (5) Mueller, J. E.; van Duin, A. C. T.; Goddard, W. A., III. Competing, Coverage-Dependent Decomposition Pathways for C_2H_2 Species on Nickel (111). *J. Phys. Chem. C* **2010**, *114*, 20028–20041.
- (6) Moskaleva, L. V.; Aleksandrov, H. A.; Basaran, D.; Zhao, Z.-J.; Rösch, N. Ethylidyne Formation from Ethylene over Pd(111): Alternative Routes from a Density Functional Study. *J. Phys. Chem. C* **2009**, *113*, 15373–15379.
- (7) Cenini, S.; La Monica, G. Organic Azides and Isocyanates as Sources of Nitrene Species in Organometallic Chemistry. *Inorg. Chim. Acta* **1976**, *18*, 279–293.
- (8) Li, Z.; Quan, R. W.; Jacobsen, E. N. Mechanism of (Diimine)copper-Catalyzed Asymmetric Aziridination of Alkenes. Nitrene Transfer via Ligand-Accelerated Catalysis. *J. Am. Chem. Soc.* **1995**, *117*, 5889–5890.
- (9) Becke, A. D. A New Mixing of Hartree–Fock and Local Density-Functional Theories. *J. Chem. Phys.* **1993**, *98*, 1372–1377.
- (10) Lee, C. T.; Yang, W. T.; Parr, R. G. Development of the Colle–Salvetti Correlation Energy Formula into a Functional of the Electron Density. *Phys. Rev. B* **1988**, *37*, 785–789.
- (11) Frisch, M. J.; et al. *Gaussian 09*, revision C.01; Gaussian, Inc.: Wallingford, CT, 2010.
- (12) Merrick, J. P.; Moran, D.; Radom, L. An Evaluation of Harmonic Vibrational Frequency Scale Factors. *J. Phys. Chem. A* **2007**, *111*, 11683–11700.
- (13) Wollman, E. W.; Kang, D.; Frisbie, C. D.; Lorkovic, I. M.; Wrighton, M. S. Photosensitive Self-Assembled Monolayers on Gold: Photochemistry of Surface-Confining Aryl Azide and Cyclopentadienylmanganese Tricarbonyl. *J. Am. Chem. Soc.* **1994**, *116*, 4395–4404.
- (14) Nakayama, T.; Inamura, K.; Inoue, Y.; Ikeda, S. Adsorption of Benzonitrile and Alkyl Cyanides on Evaporated Nickel and Palladium Films Studied by XPS. *Surf. Sci.* **1987**, *179*, 47–58.
- (15) Wu, J.-B.; Lin, Y.-F.; Wang, J.; Chang, P.-J.; Tasi, C.-P.; Lu, C.-C.; Chiu, H.-T.; Yang, Y.-W. Correlation between N 1s XPS Binding Energy and Bond Distance in Metal Amido, Imido, and Nitrido Complexes. *Inorg. Chem.* **2003**, *42*, 4516–4518.
- (16) Int1 (N6) and Int2 (N7) will be identified as surface bound NCH_2Ph and $N=CHPh$ species, respectively. The β -hydrogen elimination of Int1 is mainly responsible for the formation of Int2 ($NCH_2Ph_{(ad)} \rightarrow N=CHPh_{(ad)} + H_{(ad)}$), but the resulting surface hydrogen atoms can induce reduction of the benzonitrile (N3, N4, and N5) to afford additional Int2 ($PhC\equiv N_{(ad)} + H_{(ad)} \rightarrow N=CHPh_{(ad)}$). By including this contribution, the peak area of N7 is explicable.
- (17) NIST Chemistry WebBook. <http://webbook.nist.gov/chemistry> (accessed July 17, 2013).
- (18) Yin, J.; Krooswyk, J. D.; Hu, X.; Meyer, R. J.; Trenary, M. Formation of Benzonitrile from the Reaction of Styrene with Nitrogen on the Pt(111) Surface. *J. Phys. Chem. C* **2012**, *116*, 19300–19306.
- (19) Both the single- and two-layer metal clusters were tested in our calculations. The latter model gave more satisfactory spectral matches.
- (20) Decker, A.; Fenske, D.; Maczek, K. New Imido-Bridged Transition Metal Clusters: $[(C_5H_5)_4Ti_4(NSnMe_3)_4]$, $[Co_{11}(PPh_3)_3(NPh)_{12}]$, $[Ni_{11}Br_6(NtBu)_8]$, and $[Li(thf)_4]_4[Cu_{24}(NPh)_{14}]$. *Angew. Chem., Int. Ed.* **1996**, *35*, 2863–2866.
- (21) Albertin, G.; Antoniutti, S.; Baldan, D.; Castro, J.; Garcia-Fontán, S. Preparation of Benzyl Azide Complexes of Iridium (III). *Inorg. Chem.* **2008**, *47*, 742–748.
- (22) Zhao, J.; Hesslink, H.; Hartwig, J. F. Mechanism of β -Hydrogen Elimination from Square Planar Iridium (I) Alkoxide Complexes with Labile Dative Ligands. *J. Am. Chem. Soc.* **2001**, *123*, 7220–7227.
- (23) Hartwig, J. F. Directly-Observed β -Hydrogen Elimination of a Late Transition Metal Amido Complex and Unusual Fate of Imine Byproducts. *J. Am. Chem. Soc.* **1996**, *118*, 7010–7011.
- (24) Andrews, M. A.; Kaesz, H. D. Synthesis of Triiron Carbonyl Cluster Complexes Containing Isomeric Triply Bridging Acimidoyl or Alkylidenimido Group Derived from the Reduction of Organic Nitriles. *J. Am. Chem. Soc.* **1979**, *101*, 7238–7244.
- (25) Dawoodi, Z.; Mays, M. J.; Henrick, K. Stepwise Hydrogenation of a Nitrile on an Osmium Cluster: X-ray Crystal Structures of $[Os_3(\mu-H)(\mu-NHCH_2CF_3)(CO)_{10}]$, $[Os_3(\mu-H)_2(\mu_3-NCH_2CF_3)(CO)_9]$, and $[Os_3H(\mu-H)_3(\mu_3-NCH_2CF_3)(CO)_8]$. *J. Chem. Soc., Dalton Trans.* **1984**, 433–440.
- (26) Bernhardt, W.; Vahrenkamp, H. Stepwise Hydrogenation of Benzonitrile on a Ru_3 -Cluster. *Angew. Chem., Int. Ed.* **1984**, *23*, 381.
- (27) He, J.; Yamaguchi, K.; Mizuno, N. Aerobic Oxidative Transformation of Primary Azides to Nitriles by Ruthenium Hydroxide Catalyst. *J. Org. Chem.* **2011**, *76*, 4606–4610.
- (28) Maatta, E. A.; Du, Y. Modelling the Ammoxidation of Propylene to Acrylonitrile: The Conversion of an Allylimido(2-) Ligand to an Allylideneamido(1-) Ligand. *J. Am. Chem. Soc.* **1988**, *110*, 8249–8250.